Development 138, 1321-1327 (2011) doi:10.1242/dev.056291

RACK1 is a novel interaction partner of PTK7 that is required for neural tube closure

Peter Wehner[1,*], Iryna Shnitsar[1,3,*], Henning Urlaub[2] and Annette Borchers[1,†]

SUMMARY

RACK1 is an evolutionarily conserved intracellular adaptor protein that is involved in a wide range of processes including cell adhesion and migration; however, its role in vertebrate development is largely unknown. Here, we identify RACK1 as a novel interaction partner of PTK7, a regulator of planar cell polarity that is necessary for neural tube closure. RACK1 is likewise required for *Xenopus* neural tube closure. Further, explant assays suggest that PTK7 and RACK1 are required for neural convergent extension. Mechanistically, RACK1 is necessary for the PTK7-mediated membrane localization of Dishevelled (DSH). RACK1 facilitates the PTK7-DSH interaction by recruiting PKCδ1, a known effector of DSH membrane translocation. These data place RACK1 in a novel signaling cascade that translocates DSH to the plasma membrane and regulates vertebrate neural tube closure.

KEY WORDS: Neural tube closure, Planar cell polarity (PCP), PTK7, RACK1, Convergent extension, *Xenopus*

INTRODUCTION

A critical event in the development of the central nervous system is the formation of the neural tube from a flat neuroepithelial sheet. Neural tube closure involves a suite of highly coordinated cell shape changes and cell movements. Failure of these processes results in neural tube closure defects, which are among the most common human birth defects.

One set of genes that is known to affect neural tube closure are regulators of planar cell polarity (PCP). Mutations in mouse PCP genes lead to craniorachischisis, a severe neural tube closure defect in which the neural tube fails to close from the midbrain-hindbrain boundary to the base of the spine (Doudney and Stanier, 2005). PTK7 is a regulator of PCP that is required for neural tube closure in mouse and *Xenopus* (Lu et al., 2004), indicating an evolutionarily conserved function in this process. PTK7 is a transmembrane protein with extracellular immunoglobulin domains and a tyrosine kinase homology domain that lacks the DFG triplet necessary for catalytic activity (Kroiher et al., 2001). The signaling mechanism of PTK7 is largely unknown, but we have recently shown that PTK7 is necessary for Dishevelled (DSH) membrane localization and phosphorylation (Shnitsar and Borchers, 2008). Furthermore, our data indicate that PTK7 is part of a Frizzled 7 (FZ7)-DSH complex and is required for Frizzled 7-mediated membrane localization of DSH.

Here, we identify RACK1 (receptor of activated protein kinase C 1) as a novel interaction partner of PTK7 and show that, like PTK7, RACK1 is required for *Xenopus* neural tube closure. RACK1 is an evolutionarily conserved intracellular adaptor protein with seven tryptophan-aspartate (WD) domains that was first identified as an intracellular receptor of protein kinase C (Mochly-Rosen et al., 1991). We show that RACK1 is required for PTK7-mediated DSH localization. To our knowledge, this is the first characterization of RACK1 function during neural tube closure and PCP signaling.

MATERIALS AND METHODS

Identification of PTK7 binding partners by tandem mass spectroscopy

Myc-tagged full-length *PTK7* RNA (500 pg) or RNA coding for the kinase deletion mutant of PTK7 (*ΔkPTK7*; 300 pg) was injected into the animal pole of one-cell stage *Xenopus* embryos. Uninjected embryos were used as a control. At stage 16, 50 embryos were lysed in 500 ml NOP buffer [20 mM Tris pH 7.5, 150 mM NaCl, 0.5% NP40, supplemented with protease inhibitors (Roche), 1 mM beta-glycerol phosphate and 1 mM NaF]. All steps were performed at 4°C. Lysates were centrifuged twice for 10 minutes at 16,000 ***g*** to remove yolk proteins. Supernatants were incubated with anti-myc antibodies (Sigma, 9E10; dilution 1:500) for 1.5 hours and subsequently with Protein A Sepharose beads (Amersham) for 1 hour. Sepharose beads were washed five times with NOP buffer and the protein was released by resuspending the beads in 15 μl 4× Laemmli buffer (Invitrogen) supplemented with DTT. For mass spectrometric analysis of PTK7-associated proteins, precipitated proteins were separated by SDS-PAGE using a precast 10-15% gradient gel (Invitrogen) and stained with colloidal Coomassie Blue (Invitrogen). Single lanes were cut into 23 pieces of similar size and subjected to in-gel tryptic cleavage (Shevchenko et al., 1996). The extracted proteins were analyzed by HPLC-coupled ESI-MS/MS, which was carried out under standard conditions on a linear ion-trap mass spectrometer (4000 Qtrap; Applied Biosystems) coupled to an Agilent 1100 nanochromatography system. Peptide fragment spectra were searched against the NCBI *Xenopus* database using Mascot (Matrix Science) as a search engine.

Plasmids, RNA constructs and morpholino oligonucleotides

A *Xenopus* RACK1 (GenBank BC041541) construct was obtained from NIBB (http://Xenopus.nibb.ac.jp/; clone ID XL422i22ex). HA-tagged RACK1 was generated by PCR using 5′-GAATTCATGACTGAG-CAAATGACACTTCAG-3′ (forward) and 5′-CTCGAGACGAGTGC-CAATAGTGACCTG-3′ (reverse) primers, and inserted via *Eco*RI and *Xho*I into pCS2-HA. Human RACK1 (also known as GNB2L1) (GenBank

[1]Department of Developmental Biochemistry, Center of Molecular Physiology of the Brain (CMPB), GZMB, University of Goettingen, Justus-von-Liebig-Weg 11, 37077 Goettingen, Germany. [2]Bioanalytical Mass Spectrometry Group, Max-Planck Institute of Biophysical Chemistry, Am Fassberg 11, 37077 Goettingen, Germany. [3]Samuel Lunenfeld Research Institute, Mount Sinai Hospital, 600 University Avenue, Toronto, ON M5G 1X5, Canada.

*These authors contributed equally to this work
†Author for correspondence (annette.borchers@gmail.com)

Accepted 6 January 2011

BC032006) was obtained from Open Biosystems (IRAT40C14750184, SO#95799), and HA-tagged by PCR using 5′-AGATCGATATGACTG-AGCAGATGACCCTTCG-3′ (forward) and 5′-AAATCTAGAAAGC-GTGTGCCAATGGTCAC-3′ (reverse) primers and subsequent insertion into the pCS2-HA vector via *Cla*I and *Xba*I sites. The myc-tagged extracellular deletion mutant of PTK7, ΔEPTK7-MT, was amplified using 5′-GGAATTCCCAGACCATTGTTCTCTCTG-3′ (forward) and 5′-CGT-CTAGATCACCCTTGTGTCTTGCT-3′ (reverse) primers and inserted via *Eco*RI and *Xba*I into pCS2-myc. To generate GFP-tagged PTK7 and its kinase deletion mutant (ΔkPTK7), the myc tag was substituted by GFP via *Cla*I and *Xba*I restriction sites. The GFP was amplified from the pEGFP-C1 vector (Clontech; GenBank U55763) using 5′-ATATCGATTGGTG-AGCAAGGGCGAG-3′ (forward) and 5′-ATTCTAGACTTGTACAGCT-CGTCCATGC-3′ (reverse) primers. A fusion construct, in which the kinase domain of PTK7 was replaced by RACK1 (ΔkPTK7-R), was generated by replacing the myc tag of ΔkPTK7 (Shnitsar and Borchers, 2008) with HA-tagged RACK1. To this end, RACK1 including the HA tag was removed from RACK1-pCS2-HA with *Cla*I and *Not*I and ligated into the respective restriction sites of ΔkPTK7-pCS2-myc.

The following published plasmids were used to synthesize RNA: DSH-GFP (Yang-Snyder et al., 1996), DSH-myc (Sokol, 1996), FZ7-myc (Winklbauer et al., 2001), PKCδ1-GFP (Sivak et al., 2005) and XBF-2 (Mariani and Harland, 1998). Antisense probes for whole-mount in situ hybridization were synthesized from the following published plasmids using a DIG-RNA labeling kit (Roche): SOX2 (Mizuseki et al., 1998) and PAX3 (Bang et al., 1999). The translation-blocking morpholino oligonucleotides (MOs) for RACK1, MO1 (5′-CCCGAAGTGTCATTTG-CTCAGTCAT-3′) and MO2 (5′-CTGAAACCGCTCCACCGACTAA-GGA-3′), were generated by GeneTools. MO1 targets the ATG region, whereas MO2 targets the 5′UTR. For PTK7 loss of function, a mixture of two MOs was used (5′-TGCATCGCGGCCTCTCCCCTCA-3′ and 5′-TTCCTGCCCCGGATCCTCTCACTGC-3′) and a mixture of their 5-bp mismatches was used as a toxicity control (5′-TGgATCcCGcCCT-CTgCCgTCA-3′ and 5′-TTgCTcCCCCGcATCCTgTCAgTGC-3′). For the RACK1 loss-of-function studies, control MO (Gene Tools) or the PTK7 5-bp mismatch MO was used as a toxicity control, both giving similar results.

Xenopus microinjection, embryo manipulations and in situ hybridization

Xenopus microinjection experiments were performed as previously described (Borchers et al., 2001). Ectodermal explants (animal caps) were prepared, immunostained and analyzed as described (Shnitsar and Borchers, 2008). Whole-mount in situ hybridization was performed as described (Borchers et al., 2002; Harland, 1991).

Actin localization was visualized by phalloidin staining. Embryos were fixed in MEMFA (3.7% formaldehyde, 0.1 M MOPS, 2 mM EGTA and 1 mM $MgSO_4$) for 2 hours at room temperature, rinsed in PBS containing 0.1% Tween 20 and sectioned using a vibratome. Transverse sections were stained with 8 μg/ml fluorescent phalloidin (Sigma, P1951) conjugate solution in PBS containing 0.1% Tween 20 for 1 hour at room temperature and then rinsed three times for 10 minutes in PBS containing 0.1% Tween 20. Actin localization was analyzed using a confocal microscope.

Immunoprecipitation of in vivo and in vitro translated proteins

PTK7 and RACK1 constructs were in vitro translated using the TNT SP6 Coupled Reticulocyte Lysate System (Promega) according to the manufacturer's instructions. To test for MO specificity, the reaction was carried out in a volume of 12.5 μl with 1 μg of either RACK1 MO1, RACK1 MO2 or control MO per reaction. For immunoprecipitation, TNT lysates were diluted 1:10 with NOP buffer. Co-immunoprecipitation experiments were performed as previously described (Shnitsar and Borchers, 2008) except that anti-HA (MMS-101P, Covance) antibodies or anti-myc-coupled beads (A7470, Sigma) were used for precipitation. Precipitated proteins were detected using the following antibody dilutions: anti-MT (9E10, Sigma), 1:5000; anti-HA (MMS-101P, Covance), 1:1000; anti-GFP (11814460001, Roche), 1:1000; goat anti-mouse HRP-coupled (sc-2005, Santa Cruz Biotechnology), 1:10,000 for western blotting.

RESULTS

RACK1 interacts with PTK7 and causes neural tube closure defects

To identify PTK7 binding partners, we precipitated tagged PTK7 from *Xenopus* lysates and analyzed the co-precipitated proteins by tandem mass spectrometry. Using this approach, we isolated RACK1 as a candidate PTK7 binding partner. The interaction of RACK1 with PTK7 was verified by immunoprecipitation in *Xenopus* lysates and cell-free systems (Fig. 1A,B), indicating a direct interaction.

RACK1 and PTK7 co-expression in the closing neural tube (Kwon et al., 2001; Lu et al., 2004) and their interaction in binding assays suggest that they have a common function in neural tube closure. To analyze whether RACK1 is required for neural tube closure, two translation-blocking morpholino oligonucleotides (MOs) were used (the combination of these MOs is referred to as 'RACK1 MO' in the text). Their ability to knockdown RACK1 was verified using a radioactive in vitro translation assay (Fig. 1C). *Xenopus* embryos injected with MO1 or MO2 developed normally until neurula stages, when neural tube closure was markedly delayed compared with controls and neural folds failed to fuse in severe cases (Fig. 1D,E). The neural tube closure phenotypes were rescued by co-injection of RNA coding for human RACK1, which is not affected by MO1 (Fig. 1F,G), or by a *Xenopus* RACK1 construct lacking the MO2 binding site (Fig. 1C,H), indicating that the neural tube closure defects are caused by loss of RACK1 function. Furthermore, targeting the injection of RACK1 MO1 to the posterior neural ectoderm was sufficient to cause neural tube closure defects, demonstrating that RACK1 function is required in the neural ectoderm (see Fig. S1 in the supplementary material).

RACK1 and PTK7 are required for neural convergent extension

The RACK1 loss-of-function phenotype is highly reminiscent of the PTK7 loss-of-function phenotype and suggests that these molecules might interact to regulate neural tube closure. Time-lapse imaging of embryos injected with the RACK1 MO1 or the PTK7 MO documented a similar delay in neural tube closure (Fig. 2A). Furthermore, in situ hybridization using the pan-neural marker SOX2 and the lateral neural plate marker PAX3 demonstrated broader neural plates in these morphants (Fig. 2B), indicating defects in convergent extension of the neural plate. During convergent extension, cells intercalate along the mediolateral axis (Keller, 2002) and thereby convert the initially wide and short neural plate into a longer and thinner tissue. Defects in convergent extension cause the neural folds to form aberrantly far apart and inhibit the neural folds from meeting in the midline and fusing (Wallingford and Harland, 2002). RACK1 and PTK7 loss of function are likely to lead to convergent extension defects because the neural plate area remains wider on the RACK1 MO- or PTK7 MO-injected side than on the control side of stage 18 neurula embryos (Fig. 2C,D). Thus, these data suggest that the neural plate tissue failed to converge on the injected side.

To determine whether RACK1 and PTK7 are indeed necessary for neural convergent extension we used XBF-2-injected ectodermal explants. XBF-2 induces hindbrain and spinal cord cell fates in ectodermal explants (Mariani and Harland, 1998). This posterior neural tissue undergoes convergent extension movements leading to various degrees of explant elongation (Borchers et al., 2006; Wallingford and Harland, 2001) (Fig. 2E,F,I). Co-injection

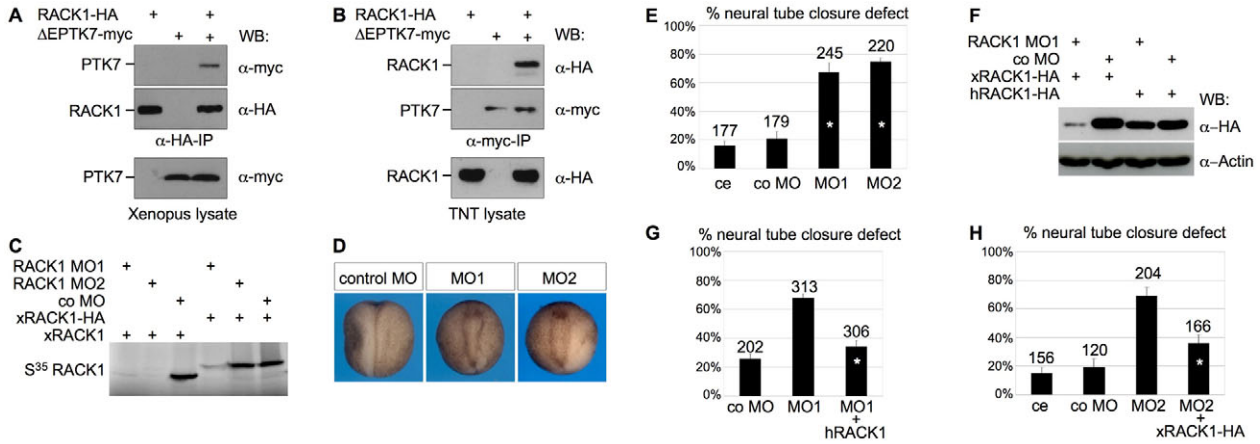

Fig. 1. RACK1 interacts with PTK7 in co-precipitation assays and is required for *Xenopus* neural tube closure. (**A**) RACK1 co-precipitates a deletion mutant of PTK7 that lacks the extracellular domain (ΔEPTK7) in lysates of embryos injected with 300 pg HA-tagged *RACK1* RNA and 500 pg myc-tagged Δ*EPTK7* RNA. WB, western blot. (**B**) In vitro translated myc-tagged ΔEPTK7 protein precipitates in vitro translated HA-tagged RACK1 protein. (**C**) RACK1 MO verification in radioactive in vitro translation assays. MO1 targets the ATG and MO2 the 5′UTR of the *Xenopus RACK1* mRNA. Both MOs inhibited the in vitro translation of full-length RACK1 containing the 5′UTR (xRACK1), whereas a control MO (co MO) did not affect protein translation. The translation of an HA-tagged RACK1 construct lacking the 5′UTR (xRACK1-HA), which contains only the MO1 binding site, is inhibited by MO1 but not MO2. The radioactive, translated RACK1 proteins (S^{35} RACK1) are shown. (**D**) Embryos injected with 20 ng MO1 or MO2 show neural tube closure defects, whereas an embryo injected with 20 ng co MO displays a closed neural tube. (**E**,**G**,**H**) Bar charts that summarize the average percentage of neural tube closure phenotypes from three independent experiments in D. The total number of injected embryos from all three batches and the s.e.m. are indicated for each condition/column. Neural tube closure defects were determined at stage 17/18. ce, uninjected control embryos. (E) Neural tube closure defects caused by 20 ng RACK1 MO1 or 20 ng MO2 are significantly different from phenotypes in embryos injected with 20 ng control MO (*, $P<0.005$, Student's *t*-test). (G) Human *RACK1* (hRACK1) RNA (300 pg) rescues the neural tube closure defects caused by 10 ng RACK1 MO1. Asterisk indicates that neural tube closure defects are significantly different from effects in embryos injected with MO1 ($P<0.005$, Student's *t*-test). (H) Injection of 300 pg *xRACK1-HA* RNA lacking the MO2 binding site rescues the neural tube closure defects caused by 20 ng MO2. Asterisk indicates neural tube closure defects significantly different from effects in embryos injected with MO2 ($P<0.01$, Student's *t*-test). (**F**) The translation of an HA-tagged *Xenopus* RACK1 construct (xRACK1) was inhibited by RACK1 MO1 but not by a control MO in *Xenopus* lysates. By contrast, the translation of an HA-tagged human RACK1 construct (hRACK1-HA) was not affected by RACK1 MO1 or the control MO. Embryos were injected at the one-cell stage with 10 ng of the respective MOs in combination with 300 pg *RACK1* RNA. At stage 11, cells were lysed and protein expression was detected by western blotting using anti-HA antibodies. Actin expression served as a loading control.

of RACK1 MO or PTK7 MO inhibited explant elongation (Fig. 2G-I), indicating that RACK1 and PTK7 are both required for neural convergent extension. Furthermore, the PTK7 MO and RACK1 MO showed additive effects, as a combination of low doses of both MOs caused the same percentage of neural tube closure defects as a high dose of the PTK7 MO (see Fig. S2A in the supplementary material).

RACK1 is required for PTK7-mediated DSH membrane recruitment

Taken together, our data suggest that PTK7 and RACK1 interact to regulate *Xenopus* neural tube closure; however, the signaling mechanism of this interaction is unclear. As we have previously shown that PTK7 functions by recruiting DSH to the plasma membrane (Shnitsar and Borchers, 2008), we analyzed whether RACK1 assists PTK7 in the membrane recruitment of DSH. If this were the case, then RACK1 should, like DSH, co-localize with PTK7 at the plasma membrane. Indeed, RACK1 was found to be localized to the cytoplasm of *Xenopus* ectodermal cells (Fig. 3A), but was recruited to the plasma membrane upon co-expression of PTK7 (Fig. 3B,D). By contrast, a kinase deletion mutant of PTK7 (ΔkPTK7), which does not recruit DSH (Shnitsar and Borchers, 2008), failed to translocate RACK1 to the plasma membrane (Fig. 3C,D). This demonstrates that the kinase domain of PTK7, which is necessary to localize DSH to the plasma membrane, is required to recruit RACK1.

Next, we examined whether RACK1 is required for the PTK7-mediated DSH localization. GFP-tagged DSH was localized in the cytoplasm of ectodermal explants (Fig. 4A), but was recruited to the plasma membrane by co-injection of myc-tagged PTK7 in the presence of a control MO (Fig. 4B,E). By contrast, RACK1 loss of function abolished the recruitment of DSH by PTK7 (Fig. 4C,E), indicating that RACK1 is required for this process. Identical results were observed for the RACK1 MO1, the RACK1 MO2 and the combination of these MOs (Fig. 4E). This effect is specific to the loss of function of RACK1, as membrane recruitment of DSH could be rescued by RACK1 constructs that are not inhibited in translation by the respective MOs (Fig. 4D,E). Thus, these data indicate that RACK1 is required for PTK7-mediated DSH recruitment.

Further, to test whether membrane recruitment of RACK1 by PTK7 is sufficient to translocate DSH to the plasma membrane, we generated a fusion construct in which the kinase domain of PTK7 was replaced by RACK1 (ΔkPTK7-R, Fig. 4F). Deletion of the kinase domain of PTK7 abolishes DSH membrane recruitment (Shnitsar and Borchers, 2008) (Fig. 4G-I,K). Interestingly, fusion of the kinase deletion mutant to RACK1 generated a protein that was able to recruit DSH (Fig. 4J,K), suggesting that the kinase domain functions by recruiting RACK1, which then leads to DSH membrane localization. Taken together, these data support a model whereby PTK7 interacts with RACK1 to localize DSH to the plasma membrane.

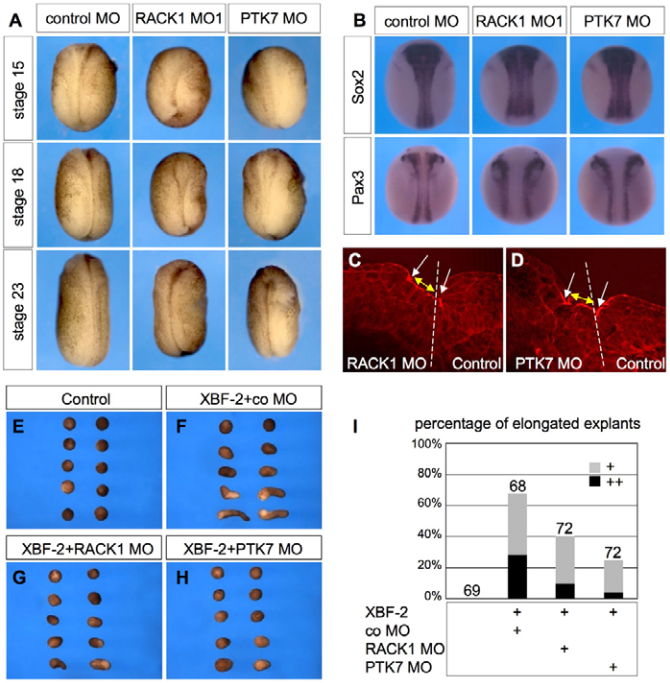

Fig. 2. RACK1 loss of function leads to similar neural tube closure defects as PTK7 loss of function. (**A**) Time-lapse images of *Xenopus* embryos injected with 10 ng control MO, RACK1 MO1 or PTK7 MO analyzed at stages 15, 18 and 23 show a similar delay in neural tube closure in the RACK1 and PTK7 morphants and the embryos remain shorter than the control. Embryos were injected at the one-cell stage and images were taken at 30-minute intervals from stage 13 to stage 23. (**B**) The expression of SOX2 (a pan-neural marker) and PAX3 (a lateral neural plate marker) is expanded in stage 17-18 embryos injected with 10 ng RACK1 MO1 or PTK7 MO compared with control MO. (**C**,**D**) Transverse sections of stage 18 embryos injected with 20 ng RACK1 MO or PTK7 MO. Embryos were injected in one blastomere at the two-cell stage; the dashed line demarcates the injected from the control side of the embryo. Phalloidin staining (red) marks the actin cytoskeleton. Actin accumulation, indicating hinge point formation (white arrows), is seen on the injected and control sides. However, the neural plate remains wide on the injected side (yellow arrow), indicating a defect in convergent extension. (**E-H**) Neural convergent extension was analyzed in ectodermal explants (animal caps) injected with 450 pg *XBF-2* RNA. Explant elongation was analyzed when control embryos reached stage 20. (E) Uninjected control caps did not elongate. (F) Explants injected with *XBF-2* and 20 ng control MO showed various degrees of elongation. (G) Co-injection of 20 ng RACK1 MO inhibited explant elongation. (H) Co-injection of 20 ng PTK7 MO inhibited elongation of explants. (**I**) The percentage of elongated explants from the experiments illustrated in E-H. Black indicates a strong elongation, gray a mild elongation. The number of explants is indicated for each condition.

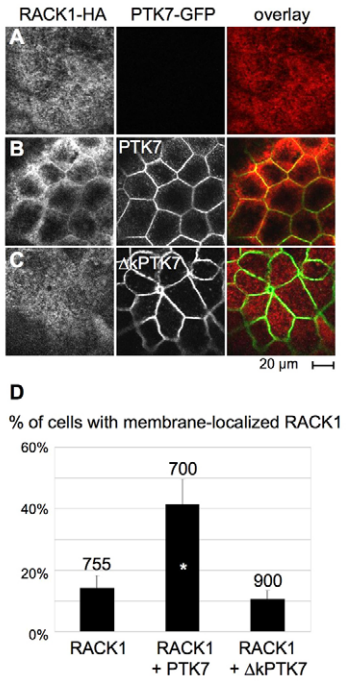

Fig. 3. PTK7 recruits RACK1 to the plasma membrane. (**A-C**) Ectodermal explants (animal caps) of blastula stage *Xenopus* embryos expressing HA-tagged RACK1 (left) and/or GFP-tagged PTK7 (middle) were analyzed by confocal microscopy. In the overlay (right), RACK1-HA fluorescence is red and PTK7-GFP is green. (A) RACK1 is localized in the cytoplasm of animal caps injected with 250 pg *RACK1-HA* RNA. (B) Co-expression of 500 pg *PTK7-GFP* RNA recruits RACK1 to the plasma membrane. (C) Deletion of the kinase domain of PTK7 abolishes membrane recruitment of RACK1. Embryos were co-injected with 250 pg *RACK1-HA* RNA and 500 pg *ΔkPTK7-GFP* RNA. (**D**) Bar chart summarizing the percentage of cells with membrane-localized RACK1 from four independent experiments in A-C. Cell number and s.e.m. are indicated for each column. Asterisk indicates that RACK1 membrane localization is significantly different from explants injected with *RACK1* mRNA.

PKCδ1 interacts with RACK1 and is required for PTK7-mediated DSH localization

RACK1 is necessary for the PTK7-mediated localization of DSH, but its role in the localization of DSH is unclear. RACK1 could function by directly interacting with DSH; however, our co-immunoprecipitation experiments did not support this hypothesis (data not shown). Since RACK1 was originally identified as a molecule that recruits active PKC (Mochly-Rosen et al., 1991), we analyzed whether the RACK1-DSH interaction is mediated by members of the PKC family. A good candidate is PKCδ1, which binds DSH and functions in a non-canonical Wnt signaling pathway regulating *Xenopus* convergent extension movements (Kinoshita et al., 2003). The interaction of RACK1 with PKCδ1 is conserved in *Xenopus*. HA-tagged *Xenopus* RACK1 co-precipitated GFP-tagged *Xenopus* PKCδ1 in lysates of neurula stage embryos (Fig. 5A). This suggests that RACK1 might interact with DSH via PKCδ1.

To examine whether the interaction with PKCδ1 is relevant for PTK7 function, we tested whether PTK7 recruits PKCδ1 to the plasma membrane and if this interaction requires RACK1. PKCδ1 was localized to the cytoplasm of *Xenopus* ectodermal explants (Fig. 5B,F) and was recruited to the plasma membrane by co-expression of PTK7 (Fig. 5C,F). However, loss of function of RACK1 abolished the PTK7-mediated PKCδ1 membrane localization (Fig. 5D,F). This effect was seen with different combinations of the RACK1 MOs and was specific to loss of function of RACK1, as it could be rescued by co-injection of human *RACK1* (Fig. 5E,F). Thus, PTK7 recruits PKCδ1 to the membrane and this process is dependent on RACK1.

Next, we analyzed whether PKCδ1 is required for the PTK7-mediated DSH localization. DSH was localized in the cytoplasm of ectodermal explants (Fig. 5G,J). Co-expression of PTK7

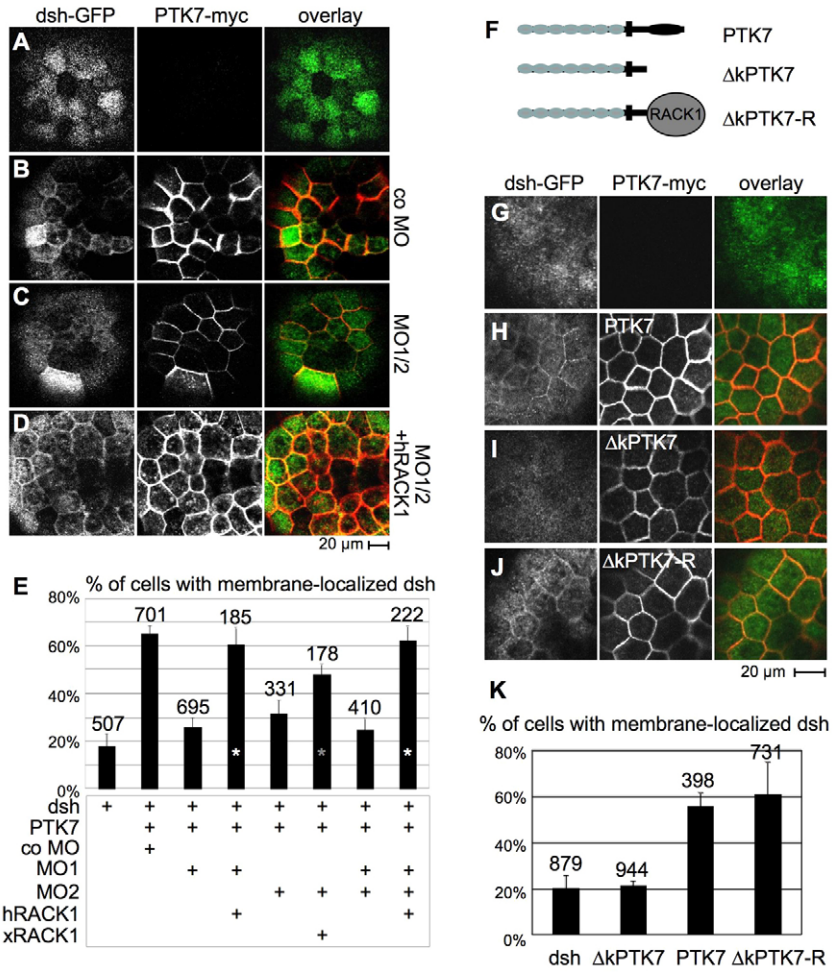

Fig. 4. RACK1 is required for PTK7-mediated DSH membrane localization. (**A-D**) *Xenopus* explants expressing GFP-tagged DSH (left) and/or myc-tagged PTK7 (middle). In the overlay (right), DSH-GFP fluorescence is green and PTK7-myc is red. (A) *Xenopus* explants injected with 100 pg *DSH-GFP* RNA express DSH mainly in the cytoplasm. (B) PTK7 translocates DSH to the plasma membrane in explants co-injected with 20 ng control MO, 500 pg *PTK7-myc* RNA and 100 pg *DSH-GFP* RNA. (C) By contrast, co-injection of 10 ng RACK1 MO1 and 10 ng RACK1 MO2 abolishes the membrane localization of DSH. (D) This effect can be rescued by co-injection of 300 pg *hRACK1* RNA. (**E**) Bar chart summarizing the percentage of cells with membrane-localized DSH from three independent experiments for each condition in A-D. Cell number and s.e.m. are indicated for each column. The asterisk indicates a significant difference between the rescue experiment and the MO injection (white, $P<0.005$; gray, $P<0.05$; Student's *t*-test). (**F**) PTK7 constructs. ΔkPTK7 lacks the kinase domain, whereas in ΔkPTK7-R the kinase domain of PTK7 is replaced by RACK1. (**G-J**) Effect of the PTK7 kinase domain constructs on DSH membrane recruitment. (G) DSH is localized in the cytoplasm of explants injected with 100 pg *DSH-GFP* RNA. (H) Co-expression of 500 pg PTK7 translocates DSH to the plasma membrane. (I) The kinase deletion mutant of PTK7 does not recruit DSH in explants injected with 300 pg *ΔkPTK7* RNA and 100 pg *DSH-GFP* RNA. (J) The fusion construct recruits DSH to the membrane. The explant was injected with 300 pg *ΔkPTK7-R* RNA and 100 pg *DSH-GFP* RNA. (**K**) Bar chart summarizing the percentage of membrane-localized DSH in explants injected with DSH and the different PTK7 constructs in G-J. Number of cells and s.e.m. are indicated for each column.

recruited DSH to the plasma membrane in the presence of control MO (Fig. 5H,J). However, co-injection of PKCδ1 MO (Kinoshita et al., 2003) abolished the membrane recruitment of DSH (Fig. 5I,J), demonstrating that PKCδ1 is required for PTK7-mediated DSH localization. Interestingly, co-injection of low doses of PTK7 MO and PKCδ1 MO led to a strong increase in neural tube closure defects, suggesting a synergistic interaction of PTK7 and PKCδ1 (see Fig. S2B in the supplementary material). Additive effects were also observed for the co-injection of PKCδ1 MO with the RACK1 MO (see Fig. S2C in the supplementary material). In summary, these data support a model whereby PTK7 recruits DSH by interacting with RACK1 and PKCδ1.

DISCUSSION

Neural tube closure defects are among the most common human birth defects, but the molecular causes have not been well defined. Here, we identify RACK1 as a novel regulator of neural tube closure and provide a mechanistic explanation for its function. In *Xenopus* embryos, RACK1 loss of function leads to defects in neural tube closure. Targeted injections and explant assays demonstrate that RACK1 is required for the convergent extension movements during neural tube closure. With respect to the signaling mechanism by which RACK1 regulates neural tube closure, we suggest that it functions by interacting with PTK7. Our data show that RACK1 and PTK7 interact in co-immunoprecipitation assays and co-localize at the plasma membrane. Furthermore, PTK7 and RACK1 loss of function both inhibit neural convergent extension in explants and whole embryos, supporting a common function in neural tube closure.

In terms of the signaling mechanism of RACK1, we propose a model in which RACK1 is required for the PTK7-mediated membrane localization of DSH. Previously, we have shown that PTK7 is required for the membrane recruitment of DSH (Shnitsar and Borchers, 2008), a prerequisite for the activation of non-canonical Wnt signaling (Park et al., 2005). Here, we show that PTK7 directly interacts with RACK1 and recruits it to the plasma membrane. Furthermore, PTK7 requires RACK1 to bring DSH to the plasma membrane. RACK1 is likely to participate in DSH membrane recruitment through the interaction with PKCδ1. Indeed, our data show that PTK7 recruits PKCδ1 to the plasma membrane and that RACK1 is required for this function. PKCδ1 is also crucial for PTK7-mediated DSH localization, as PKCδ1 loss of function inhibits DSH recruitment by PTK7. PKCδ1 might affect DSH localization simply by mediating protein binding or through mechanisms involving its kinase activity. In summary, these data suggest a model in which PTK7, RACK1 and PKCδ1 cooperate to recruit DSH to the plasma membrane.

DSH membrane localization has been attributed to the activation of non-canonical Wnt signaling and can be facilitated by members of the Frizzled family (Axelrod et al., 1998; Medina and Steinbeisser, 2000; Rothbacher et al., 2000) or by PTK7, as our data suggest. We have previously shown that PTK7 forms a

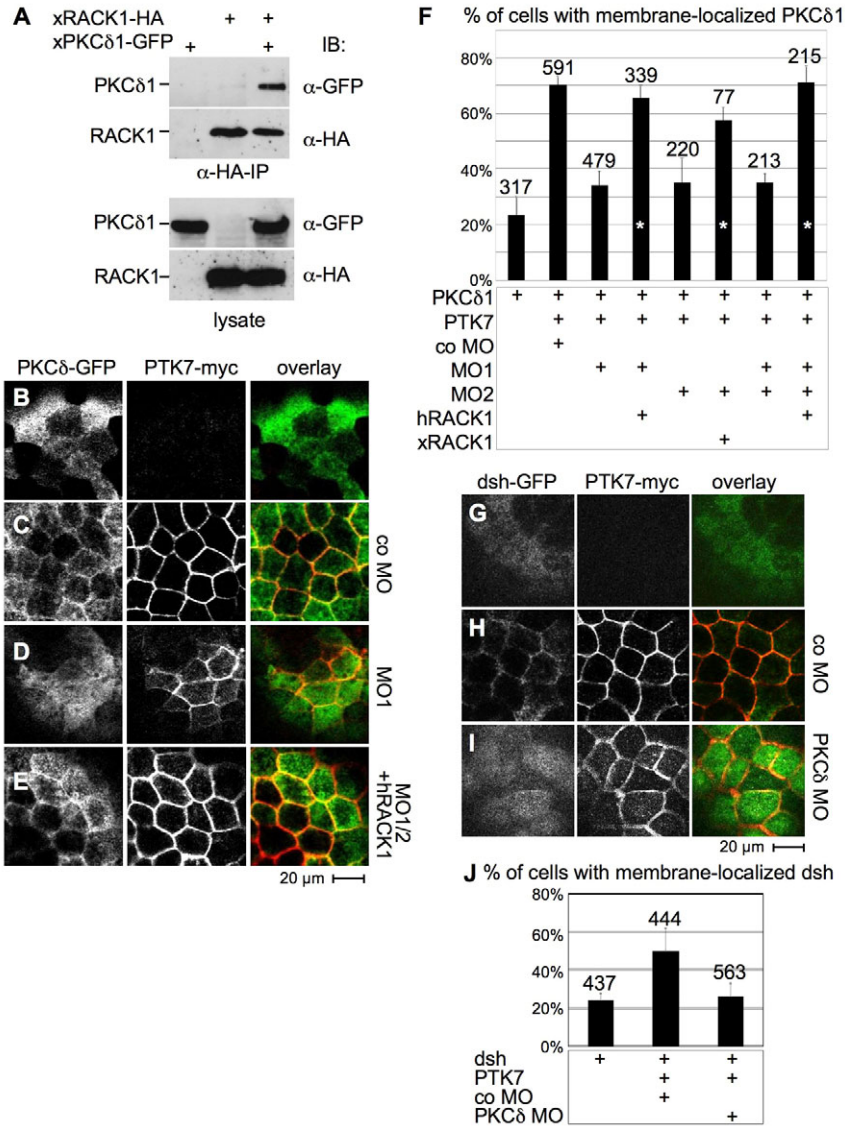

Fig. 5. PTK7 recruits DSH via RACK1 and PKCδ1. (**A**) HA-tagged RACK1 precipitates GFP-tagged PKCδ1 in *Xenopus* lysates injected with 300 pg *RACK1-HA* RNA and 500 pg *PKCδ1-GFP* RNA. (**B-E**) Animal cap localization assay showing co-localization of myc-tagged PTK7 (middle, red in overlay) with GFP-tagged PKCδ1 (left, green in overlay). (B) GFP-tagged PKCδ1 is localized in the cytoplasm of animal caps injected with 250 pg *PKCδ1-GFP* RNA. (C) Co-expression of myc-tagged PTK7 recruits GFP-tagged PKCδ1 to the plasma membrane in the presence of a control MO. Animal caps were injected with 700 pg *PTK7-myc* RNA, 250 pg *PKCδ1-GFP* RNA and 20 ng control MO. (D) Co-injection of 20 ng RACK1 MO1 inhibits the PTK7-mediated PKCδ1 membrane recruitment. (E) Membrane localization can be rescued by co-injection of 300 pg *hRACK1* RNA with RACK1 MO1 and MO2. (**F**) Bar chart summarizing the percentage of membrane-recruited PKCδ1 in B-E. Number of analyzed cells and s.e.m. are indicated. Asterisk indicates a significant difference between the rescue experiment and the MO injection ($P<0.05$, Student's *t*-test). (**G-I**) Animal cap localization assay showing co-localization of GFP-tagged DSH (left, green in overlay) with myc-tagged PTK7 (middle, red in overlay). (G) Explants injected with 100 pg *DSH-GFP* RNA express DSH mainly in the cytoplasm. (H) PTK7 translocates DSH to the plasma membrane in explants co-injected with 20 ng control MO, 500 pg *PTK7-myc* RNA and 100 pg *DSH-GFP* RNA. (I) Co-injection of 20 ng PKCδ MO inhibits the PTK7-mediated DSH membrane recruitment. (**J**) Bar chart summarizing the percentage of cells with membrane-localized *DSH*-GFP in G-I. Number of analyzed cells and s.e.m. are indicated.

complex with FZ7 and DSH and is required for the FZ7-mediated membrane localization and hyperphosphorylation of DSH (Shnitsar and Borchers, 2008); however, it seems that RACK1 is not required for this process. First, FZ7 does not recruit RACK1 to the plasma membrane (data not shown). Second, RACK1 is not required for FZ7-mediated DSH membrane localization or hyperphosphorylation of DSH (see Fig. S3 in the supplementary material). Therefore, our data indicate that RACK1 does not function in the FZ7-mediated membrane localization of DSH. These data seem to contradict our previous findings, in which we showed that PTK7 is required for FZ7-mediated DSH recruitment (Shnitsar and Borchers, 2008). An explanation is that PTK7, independent of its ability to recruit DSH (via a mechanism that requires RACK1), stabilizes the FZ7-DSH complex. Loss of function of PTK7 leads to destabilization of this complex, thereby affecting the ability of FZ7 to recruit DSH. Notably, loss of function of FZ7 does not inhibit PTK7-mediated DSH localization (data not shown), supporting the hypothesis that PTK7 recruits DSH via an FZ7-independent mechanism. Thus, we favor a model in which PTK7 recruits DSH via a RACK1-dependent mechanism but affects the FZ7-DSH interaction by a different mechanism, possibly by stabilizing the complex in a Wnt-dependent manner.

It is likely that PTK7 and FZ7 represent parallel molecular mechanisms to recruit DSH, but they might activate distinct downstream signaling events. The downstream signaling events of the PTK7-RACK1 interaction are currently unclear, but it is tempting to speculate that it could affect JNK signaling. This hypothesis is supported by the finding that PTK7 leads to an increase in JNK phosphorylation (Shnitsar and Borchers, 2008). Furthermore, RACK1 functions as an adaptor for PKC-mediated JNK activation (Lopez-Bergami et al., 2005). A future challenge will be to further dissect the downstream signaling events leading to neural tube closure.

Acknowledgements
We thank H. Steinbeisser for providing plasmids; A. Wodarz for supplying the laser scanning microscope; I. Wunderlich for technical support; and T. Pieler for providing the infrastructure. This work was funded by grants to A.B. by the Deutsche Forschungsgemeinschaft (DFG) and the DFG Center for Molecular Physiology of the Brain (CMPB).

Competing interests statement
The authors declare no competing financial interests.

Supplementary material
Supplementary material for this article is available at
http://dev.biologists.org/lookup/suppl/doi:10.1242/dev.056291/-/DC1

References

Axelrod, J. D., Miller, J. R., Shulman, J. M., Moon, R. T. and Perrimon, N. (1998). Differential recruitment of Dishevelled provides signaling specificity in the planar cell polarity and Wingless signaling pathways. *Genes Dev.* **12**, 2610-2622.

Bang, A. G., Papalopulu, N., Goulding, M. D. and Kintner, C. (1999). Expression of Pax-3 in the lateral neural plate is dependent on a Wnt-mediated signal from posterior nonaxial mesoderm. *Dev. Biol.* **212**, 366-380.

Borchers, A., David, R. and Wedlich, D. (2001). Xenopus cadherin-11 restrains cranial neural crest migration and influences neural crest specification. *Development* **128**, 3049-3060.

Borchers, A. G., Hufton, A. L., Eldridge, A. G., Jackson, P. K., Harland, R. M. and Baker, J. C. (2002). The E3 ubiquitin ligase GREUL1 anteriorizes ectoderm during Xenopus development. *Dev. Biol.* **251**, 395-408.

Borchers, A., Fonar, Y., Frank, D. and Baker, J. C. (2006). XNF-ATc3 affects neural convergent extension. *Development* **133**, 1745-1755.

Doudney, K. and Stanier, P. (2005). Epithelial cell polarity genes are required for neural tube closure. *Am. J. Med. Genet. C Semin. Med. Genet.* **135C**, 42-47.

Harland, R. M. (1991). In situ hybridization: an improved whole-mount method for Xenopus embryos. *Methods Cell Biol.* **36**, 685-695.

Keller, R. (2002). Shaping the vertebrate body plan by polarized embryonic cell movements. *Science* **298**, 1950-1954.

Kinoshita, N., Iioka, H., Miyakoshi, A. and Ueno, N. (2003). PKC delta is essential for Dishevelled function in a noncanonical Wnt pathway that regulates Xenopus convergent extension movements. *Genes Dev.* **17**, 1663-1676.

Kroiher, M., Miller, M. A. and Steele, R. E. (2001). Deceiving appearances: signaling by 'dead' and 'fractured' receptor protein-tyrosine kinases. *BioEssays* **23**, 69-76.

Kwon, H. J., Bae, S., Son, Y. H. and Chung, H. M. (2001). Expression of the Xenopus homologue of the receptor for activated C-kinase 1 (RACK1) in the Xenopus embryo. *Dev. Genes Evol.* **211**, 195-197.

Lopez-Bergami, P., Habelhah, H., Bhoumik, A., Zhang, W., Wang, L. H. and Ronai, Z. (2005). RACK1 mediates activation of JNK by protein kinase C. *Mol. Cell* **19**, 309-320.

Lu, X., Borchers, A. G., Jolicoeur, C., Rayburn, H., Baker, J. C. and Tessier-Lavigne, M. (2004). PTK7/CCK-4 is a novel regulator of planar cell polarity in vertebrates. *Nature* **430**, 93-98.

Mariani, F. V. and Harland, R. M. (1998). XBF-2 is a transcriptional repressor that converts ectoderm into neural tissue. *Development* **125**, 5019-5031.

Medina, A. and Steinbeisser, H. (2000). Interaction of Frizzled 7 and Dishevelled in Xenopus. *Dev. Dyn.* **218**, 671-680.

Mizuseki, K., Kishi, M., Matsui, M., Nakanishi, S. and Sasai, Y. (1998). Xenopus Zic-related-1 and Sox-2, two factors induced by chordin, have distinct activities in the initiation of neural induction. *Development* **125**, 579-587.

Mochly-Rosen, D., Khaner, H. and Lopez, J. (1991). Identification of intracellular receptor proteins for activated protein kinase C. *Proc. Natl. Acad. Sci. USA* **88**, 3997-4000.

Park, T. J., Gray, R. S., Sato, A., Habas, R. and Wallingford, J. B. (2005). Subcellular localization and signaling properties of dishevelled in developing vertebrate embryos. *Curr. Biol.* **15**, 1039-1044.

Rothbacher, U., Laurent, M. N., Deardorff, M. A., Klein, P. S., Cho, K. W. and Fraser, S. E. (2000). Dishevelled phosphorylation, subcellular localization and multimerization regulate its role in early embryogenesis. *EMBO J.* **19**, 1010-1022.

Shevchenko, A., Wilm, M., Vorm, O. and Mann, M. (1996). Mass spectrometric sequencing of proteins silver-stained polyacrylamide gels. *Anal. Chem.* **68**, 850-858.

Shnitsar, I. and Borchers, A. (2008). PTK7 recruits dsh to regulate neural crest migration. *Development* **135**, 4015-4024.

Sivak, J. M., Petersen, L. F. and Amaya, E. (2005). FGF signal interpretation is directed by Sprouty and Spred proteins during mesoderm formation. *Dev. Cell* **8**, 689-701.

Sokol, S. Y. (1996). Analysis of Dishevelled signalling pathways during Xenopus development. *Curr. Biol.* **6**, 1456-1467.

Wallingford, J. B. and Harland, R. M. (2001). Xenopus Dishevelled signaling regulates both neural and mesodermal convergent extension: parallel forces elongating the body axis. *Development* **128**, 2581-2592.

Winklbauer, R., Medina, A., Swain, R. K. and Steinbeisser, H. (2001). Frizzled-7 signalling controls tissue separation during Xenopus gastrulation. *Nature* **413**, 856-860.

Yang-Snyder, J., Miller, J. R., Brown, J. D., Lai, C. J. and Moon, R. T. (1996). A frizzled homolog functions in a vertebrate Wnt signaling pathway. *Curr. Biol.* **6**, 1302-1306.